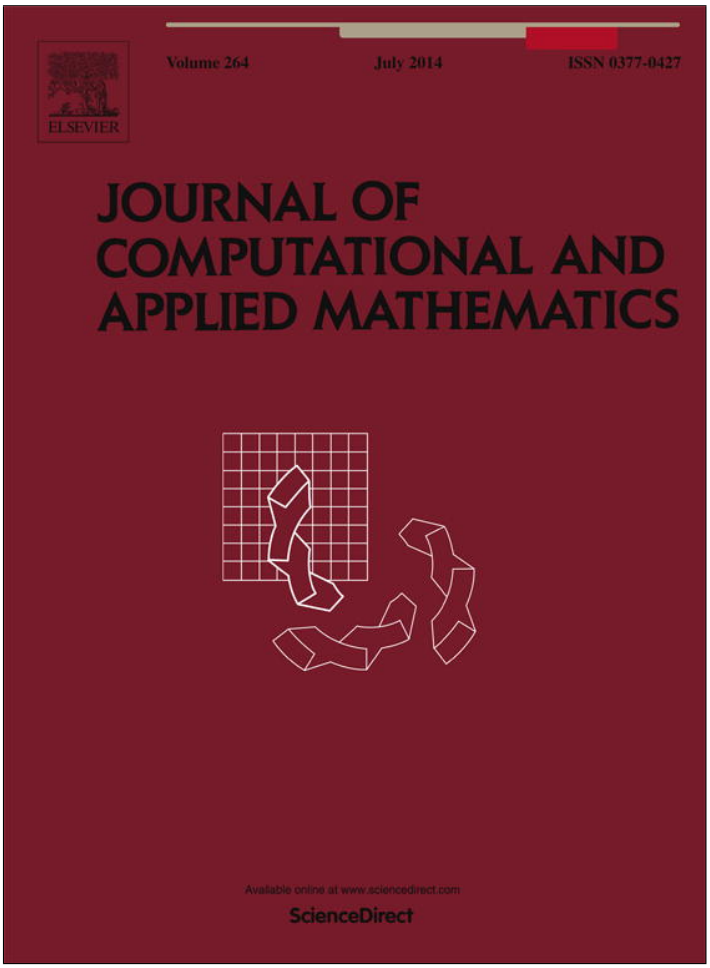

Journal of Computational and Applied Mathematics 264 (2014) 99–114

Contents lists available at ScienceDirect

Journal of Computational and Applied Mathematics

journal homepage: www.elsevier.com/locate/cam

Elastoplastic analysis by active macro-zones with linear kinematic hardening and von Mises materials

L. Zito, S. Terravecchia, T. Panzeca *

D.to di Ingegneria Civile, Ambientale e Aerospaziale, Università di Palermo, viale delle Scienze, 90128 Palermo, Italy

ARTICLE INFO

Article history:
Received 4 March 2011
Received in revised form 7 January 2013

Keywords:
Multidomain SGBEM
Self-equilibrium stress
Active macro-zones
Hardening von Mises materials
Return mapping algorithm

ABSTRACT

In this paper a strategy to perform elastoplastic analysis with linear kinematic hardening for von Mises materials under plane strain conditions is shown. The proposed approach works with the Symmetric Galerkin Boundary Element Method applied to multidomain problems using a mixed variables approach, to obtain a more stringent solution. The elastoplastic analysis is carried out as the response to the loads and the plastic strains, the latter evaluated through the self-equilibrium stress matrix. This matrix is used both, in the predictor phase, for trial stress evaluation and, in the corrector phase, for solving a nonlinear global system which provides the elastoplastic solution of the active macro-zones, i.e. those zones collecting bem-elements where the plastic consistency condition has been violated.

The simultaneous use of active macro-zones gives rise to a nonlocal approach which is characterized by a large decrease in the plastic iteration number, although the proposed strategy requires the inversion and updating of Jacobian operators generally of big dimensions. A strategy developed in order to reduce the computational efforts due to the use of this matrix, in a recursive process, is shown.

1. Introduction

The present paper shows a Symmetric Galerkin Boundary Element Method (SGBEM) using a mixed variables multidomain approach [1] in initial strain elastoplastic 2D problems, in the hypothesis of von Mises materials, associated flow rule, plane strain state and linear kinematic hardening behaviour.

In the past, in the BEM context, the elastoplastic analysis was dealt with using the collocation approach: we can mention the papers by Aliabadi and Martin [2] dealing with the contact problem, Hatzigeorgeou and Beskos [3] in dynamics through 3D inner discretization, Ribeiro et al. [4] through generation of cells introduced during the analysis process, Brebbia et al. [5] and the numerous researches inserted in the relevant references to the authors cited.

Differently, the present approach utilizes the symmetric BEM and starts from the discretization of the domain into substructures, called bem-elements (bem-e), where the plastic strains stored in discrete terms have to be computed. The idea of subdividing the domain into substructures was introduced in the SGBEM by Maier et al. [6] through a variational approach. Subsequently Gray and Paulino [7] utilized substructuring in potential problems; Layton et al. [8] proposed a formulation dividing the body into macroelements, each of which is governed by boundary quantities only, obtaining inside a condensation process a system having some non-symmetric blocks; Ganguly et al. [9] presented an entirely symmetric approach for a plane elastic body subdivided by two macroelements, discretized along the boundary and characterized by a symmetric solving system having as unknowns the boundary quantities of both the macroelements.

* Corresponding author. Tel.: +39 91 23896753; fax: +39 91 6568407.
E-mail address: tpanzeca@tiscali.it (T. Panzeca).

0377-0427/$ – see front matter © 2014 Elsevier B.V. All rights reserved.
http://dx.doi.org/10.1016/j.cam.2014.01.008

Panzeca et al. dealt with the same problem by using a strategy connected to the SGBEM variational formulation introduced by Maier and Polizzotto [10] and Polizzotto [11,12], and obtained two different multidomain approaches defined as mixed variable approach [13] and displacement one [14,15], both characterized by strong variable condensation, numerically compared by Terravecchia [16] inside an elastic analysis. Through these strategies the authors obtained an equation system only depending on the interface nodal variables of the contiguous bem-elements.

The mixed variables multidomain approach was developed as a natural evolution of the displacements approach [15], applied by the same research group in some mechanics problems like thermoelasticity [17], the contact-detachment problem [18], the mechanics of quasi-brittle fracture [19] and ideal elastoplasticity [20]. The approaches guarantee the compatibility and equilibrium at all the points of the domain, but only in weighted form along the boundary elements as a consequence of the discretization.

The strategy contemplates the evaluation, for each bem-e, of expressions which relate mechanical and kinematical weighted quantities in the interface boundaries and stresses evaluated at Gauss points to mechanical and kinematical nodal quantities defined in the same interface boundaries, and to the boundary (forces and imposed displacements) and domain (body forces and plastic strains) actions. These expressions, written for every bem-e, are characterized by elastic operators containing the geometry and constitutive data.

The governing equation is obtained by imposing the regularity conditions between bem-elements regarding the kinematical and mechanical quantities both in terms of nodal variables (strong regularity) and in terms of generalized ones (weak regularity).

This procedure uses a self-equilibrium stresses equation [21,22] governing the elastoplastic problem and relates stresses, valuated at the Gauss points, to stored plastic strains through an influence matrix (self-stress matrix) which is non-symmetric, negative semi-definite and fully-populated.

Inside a step-by-step load process, within which the elastoplastic analysis is considered path-independent, this matrix makes it possible to perform the predictor phase, and therefore it locates all the active bem-elements, and as a consequence defines the active macro-zones.

Then, in a subsequent phase, the elastic solution is corrected by a return mapping algorithm. The proposed strategy permits the simultaneous correction of the elastic solution in all the active bem-elements and utilizes the same self-equilibrium stresses matrix, changed in sign, in a nonlinear system having the end-step stresses, the internal variables (back stresses) and the plastic multiplier increments as unknowns. In the present approach the approximate solution of the previous nonlinear problem is obtained by the well-known Newton–Raphson procedure (N–R), utilized for Bem formulations by several authors [23–27].

The strategy shows considerable computational advantages: the low number of unknowns in the elastic analysis, the reduced number of plastic iterations (three or four for any load step), and the updating of the plastic strains in the bem-elements through the employment of a nonlocal strategy where the plastic strains are stored simultaneously in all the active bem-elements. The operative difficulties arise from the large dimension of the Jacobian operator, but in this paper for its inversion a strategy to reduce the computational efforts is shown.

Moreover the present approach offers the advantages of updating the nodal unknowns caused by plastic actions only at the end of single load step and directly obtaining a path-independent elastoplastic solution.

This paper shows some characteristics of the elastoplastic analysis dealt with the SGBEM using the active macro-zones, in two previous papers by some of the present authors. In the first paper [28] the elastoplastic analysis is carried out through the so-called "displacement method" of the SGBEM, where the constitutive model of the material is elastic-perfectly plastic. In the second one [29] the elastic-perfectly plastic analysis is dealt with as a limit analysis, performed in a canonical form as a convex optimization problem with quadratic constraints, in terms of discrete variables, and implemented with the Karnak.sGbem code coupled with the optimization toolbox by MatLab.

Some examples are shown using the Karnak.sGbem analysis code [30], by which it was possible to make some comparisons with other approaches for the purpose of showing the effectiveness of the proposed method.

2. Self-stress equation via multidomain SGBEM

This section shows a detailed description of the procedure utilized to obtain, using the SGBEM applied to multidomain problems, an elasticity equation connecting the stresses to the plastic strains through a stiffness matrix involving all the bem-elements of the discretized system.

Consider the classical Somigliana Identities (S.Is.):

$$\mathbf{u} = \int_{\Gamma} \mathbf{G}_{uu}\mathbf{f}\, d\Gamma + \int_{\Gamma} \mathbf{G}_{ut}(-\mathbf{u})\, d\Gamma + \int_{\Omega} \mathbf{G}_{u\sigma}\boldsymbol{\varepsilon}^{p} d\Omega \tag{1a}$$

$$\mathbf{t} = \int_{\Gamma} \mathbf{G}_{tu}\mathbf{f}\, d\Gamma + \int_{\Gamma} \mathbf{G}_{tt}(-\mathbf{u})\, d\Gamma + \int_{\Omega} \mathbf{G}_{t\sigma}\boldsymbol{\varepsilon}^{p} d\Omega \tag{1b}$$

$$\boldsymbol{\sigma} = \int_{\Gamma} \mathbf{G}_{\sigma u}\mathbf{f}\, d\Gamma + \int_{\Gamma} \mathbf{G}_{\sigma t}(-\mathbf{u})\, d\Gamma + \int_{\Omega} \mathbf{G}_{\sigma\sigma}\boldsymbol{\varepsilon}^{p} d\Omega. \tag{1c}$$

These provide the displacements, tractions and stresses in the unbounded domain caused by layered mechanical jumps $\mathbf{f}$ and double-layered kinematical ones $-\mathbf{u}$ as well as by volumetric inelastic actions $\boldsymbol{\varepsilon}^p$ in Ω domain. The operators $\mathbf{G}_{pq}$ are the Fundamental Solution matrices, whose symbology was introduced by Maier and Polizzotto [10]; the subindices $p = u,\ t,\ \sigma$ and $q = u,\ t,\ \sigma$ indicate the effect and the dual quantity in an energetic sense associated with the cause, respectively.

Consider a bi-dimensional body having domain Ω and boundary Γ, subjected to actions acting in its plane:

- forces $\bar{\mathbf{f}}_2$ at the portion Γ_2 of free boundary,
- displacements $\bar{\mathbf{u}}_1$ imposed at the portion Γ_1 of constrained boundary,
- plastic strains $\boldsymbol{\varepsilon}^p$ in Ω.

In the hypothesis that the physical and geometrical characteristics of the body are zone-wise variables, an appropriate subdivision of the domain into bem-elements is introduced. This subdivision involves the introduction of interface boundaries Γ_0 between contiguous bem-elements.

We want to obtain the elastic response to the external actions in terms of displacements $\mathbf{u}_2$ on Γ_2 and reactive forces $\mathbf{f}_1$ on Γ_1, but also in terms of the displacements $\mathbf{u}_0$ and tractions $\mathbf{t}_0$ on the interface boundary Γ_0 and of the stresses $\boldsymbol{\sigma}$ in the domain of each bem-element by using the mixed variables multidomain SGBEM approach [13]. Eqs. (1a) and (1b) are utilized in order to obtain, through the employment of weighted quantities, the algebraic operator coefficients necessary to perform the analysis phase; Eq. (1c) is utilized to provide the stress state at the Gauss points of the bem-elements in the post-processing phase employing the self-stresses equation.

2.1. Governing equations of the bem-e

Consider a generic bem-e, characterized by the boundary Γ distinguished into three parts, free Γ_2, constrained Γ_1 and interface Γ_0, but generally not all present. For this bem-e the following Dirichlet and Neumann conditions may be written:

$$\mathbf{u}_1 = \bar{\mathbf{u}}_1 \quad \text{on } \Gamma_1 \tag{2a}$$

$$\mathbf{t}_2 = \bar{\mathbf{f}}_2 \quad \text{on } \Gamma_2. \tag{2b}$$

If we introduce in Eqs. (2a) and (2b) the S.I. of the displacements and tractions, the following boundary integral equations may be obtained:

$$\mathbf{u}_1[\mathbf{f}_1, -\mathbf{u}_2, \mathbf{f}_0, -\mathbf{u}_0] + \mathbf{u}_1[\boldsymbol{\varepsilon}^p] + \mathbf{u}_1[\bar{\mathbf{f}}_2, -\bar{\mathbf{u}}_1^{PV}] + \frac{1}{2}\bar{\mathbf{u}}_1 = \bar{\mathbf{u}}_1 \tag{3a}$$

$$\mathbf{t}_2[\mathbf{f}_1, -\mathbf{u}_2, \mathbf{f}_0, -\mathbf{u}_0] + \mathbf{t}_2[\boldsymbol{\varepsilon}^p] + \mathbf{t}_2[\bar{\mathbf{f}}_2^{PV}, -\bar{\mathbf{u}}_1] + \frac{1}{2}\bar{\mathbf{f}}_2 = \bar{\mathbf{f}}_2 \tag{3b}$$

where a symbolic form has been used and where the typologies of the boundary are characterized by the indices introduced in the displacement and traction vectors.

It is necessary to define the unknowns $\mathbf{u}_0$ and $\mathbf{t}_0$, related to the interface boundary Γ_0

$$\mathbf{u}_0 = \mathbf{u}_0[\mathbf{f}_1, -\mathbf{u}_2, \mathbf{f}_0, -\mathbf{u}_0^{PV}] + \frac{1}{2}\mathbf{u}_0 + \mathbf{u}_0[\boldsymbol{\varepsilon}^p] + \mathbf{u}_0[\bar{\mathbf{f}}_2, -\bar{\mathbf{u}}_1] \tag{4a}$$

$$\mathbf{t}_0 = \mathbf{t}_0[\mathbf{f}_1, -\mathbf{u}_2, \mathbf{f}_0^{PV}, -\mathbf{u}_0] + \frac{1}{2}\mathbf{t}_0 + \mathbf{t}_0[\boldsymbol{\varepsilon}^p] + \mathbf{t}_0[\bar{\mathbf{f}}_2, -\bar{\mathbf{u}}_1] \tag{4b}$$

and to introduce the stress field in the domain Ω:

$$\boldsymbol{\sigma} = \boldsymbol{\sigma}\ [\mathbf{f}_1, -\mathbf{u}_2, \mathbf{f}_0, -\mathbf{u}_0] + \boldsymbol{\sigma}[\boldsymbol{\varepsilon}^p] + \boldsymbol{\sigma}\ [\bar{\mathbf{f}}_2, -\bar{\mathbf{u}}_1] \tag{5}$$

where the terms $\mathbf{u}[-\mathbf{u}^{PV}]$ and $\mathbf{t}[\mathbf{t}^{PV}]$ define the presence of integrals as the Cauchy Principal Values, and the terms where 1/2 occurs are the corresponding free terms.

Eqs. (3a) and (3b) have to be rewritten in a different way

$$\mathbf{u}_1[\mathbf{f}_1, -\mathbf{u}_2, \mathbf{f}_0, -\mathbf{u}_0] + \mathbf{u}_1[\boldsymbol{\varepsilon}^p] + \underbrace{\mathbf{u}_1[\bar{\mathbf{f}}_2, -\bar{\mathbf{u}}_1^{PV}] - \frac{1}{2}\bar{\mathbf{u}}_1}_{\hat{\mathbf{u}}_1} = \mathbf{0} \tag{6a}$$

$$\mathbf{t}_2[\mathbf{f}_1, -\mathbf{u}_2, \mathbf{f}_0, -\mathbf{u}_0] + \mathbf{t}_2[\boldsymbol{\varepsilon}^p] + \underbrace{\mathbf{t}_2[\bar{\mathbf{f}}_2^{PV}, -\bar{\mathbf{u}}_1] - \frac{1}{2}\bar{\mathbf{f}}_2}_{\hat{\mathbf{t}}_2} = \mathbf{0} \tag{6b}$$

whereas Eqs. (4a), (4b) and (5) remain unchanged.

In the previous integral equations (4), (6) and (5), $\boldsymbol{\varepsilon}^p$ is the plastic strain vector, whose evaluation strategy is defined in the next section.

We introduce the boundary discretization into the boundary elements by performing the following modelling of all the known and unknown quantities:

$$\mathbf{f}_1 = \boldsymbol{\Psi}_t\ \mathbf{F}_1, \tag{7a}$$

$$\bar{\mathbf{f}}_2 = \boldsymbol{\Psi}_t\ \bar{\mathbf{F}}_2, \tag{7b}$$

$$\mathbf{t}_0 = \boldsymbol{\Psi}_t\ \mathbf{F}_0, \tag{7c}$$

$$\mathbf{u}_2 = \boldsymbol{\Psi}_u\ \mathbf{U}_2, \tag{7d}$$

$$\bar{\mathbf{u}}_1 = \boldsymbol{\Psi}_u\ \bar{\mathbf{U}}_1, \tag{7e}$$

$$\mathbf{u}_0 = \boldsymbol{\Psi}_u\ \mathbf{U}_0, \tag{7f}$$

$$\boldsymbol{\varepsilon}^p = \boldsymbol{\Psi}_p\ \mathbf{p} \tag{7g}$$

where $\boldsymbol{\Psi}_t$ and $\boldsymbol{\Psi}_u$ are appropriate matrices of shape functions regarding the boundary quantities, while $\boldsymbol{\Psi}_p$ are domain shape functions used to model the volumetric plastic strains. Further, the capital letters indicate the nodal vectors of the forces ($\mathbf{F}_1$, $\bar{\mathbf{F}}_2$ and $\mathbf{F}_0$) and of the displacements ($\bar{\mathbf{U}}_1$, $\mathbf{U}_2$ and $\mathbf{U}_0$) defined on the boundary nodes.

We now perform the weighting of all the coefficients of Eqs. (4) and (6). For this purpose, the same shape functions as those modelling the causes are employed, but introduced in an energetically dual way in according to the Galerkin approach [10], thus obtaining the following generalized equations:

$$\int_{\Gamma_1} \boldsymbol{\psi}_f^T(\mathbf{u}_1 - \bar{\mathbf{u}}_1) = \mathbf{0}, \tag{8a}$$

$$\int_{\Gamma_2} \boldsymbol{\psi}_u^T(\mathbf{t}_2 - \bar{\mathbf{f}}_2) = \mathbf{0}, \tag{8b}$$

$$\mathbf{W}_0 = \int_{\Gamma_0} \boldsymbol{\psi}_f^T \mathbf{u}_0, \tag{8c}$$

$$\mathbf{P}_0 = \int_{\Gamma_0} \boldsymbol{\psi}_u^T \mathbf{t}_0. \tag{8d}$$

As a consequence, Eqs. (8a)–(8d) and (5) are rewritten in the following symbolic form:

$$\left.\begin{aligned}
&\mathbf{W}_1[\mathbf{F}_1, -\mathbf{U}_2, \mathbf{F}_0, -\mathbf{U}_0] + \mathbf{W}_1[\mathbf{p}] + \beta\,\hat{\mathbf{W}}_1 = \mathbf{0}\\
&\mathbf{P}_2[\mathbf{F}_1, -\mathbf{U}_2, \mathbf{F}_0, -\mathbf{U}_0] + \mathbf{P}_2[\mathbf{p}] + \beta\,\hat{\mathbf{P}}_2 = \mathbf{0}\\
&\mathbf{W}_0 = \mathbf{W}_0[\mathbf{F}_1, -\mathbf{U}_2, \mathbf{F}_0, -\mathbf{U}_0] + \mathbf{W}_0[\mathbf{p}] + \beta\,\hat{\mathbf{W}}_0\\
&\mathbf{P}_0 = \mathbf{P}_0[\mathbf{F}_1, -\mathbf{U}_2, \mathbf{F}_0, -\mathbf{U}_0] + \mathbf{P}_0[\mathbf{p}] + \beta\,\hat{\mathbf{P}}_0
\end{aligned}\right\}\ \textit{Symmetric BEM}$$

$$\left.\boldsymbol{\sigma} = \boldsymbol{\sigma}[\mathbf{F}_1, -\mathbf{U}_2, \mathbf{F}_0, -\mathbf{U}_0] + \boldsymbol{\sigma}[\mathbf{p}] + \beta\,\hat{\mathbf{I}}_\sigma\right\}\ \textit{Collocation BEM} \tag{9a–e}$$

where the load multiplier β of the external actions has been introduced.

In this way it is possible to obtain the following block system regarding Eq. (9):

$$\left|\begin{array}{c}\mathbf{0}\\ \mathbf{0}\\ \hline \mathbf{W}_0\\ \mathbf{P}_0\end{array}\right| = \left|\begin{array}{cc|cc} \mathbf{A}_{u1u1} & \mathbf{A}_{u1f2} & \mathbf{A}_{u1u0} & \mathbf{A}_{u1f0}\\ \mathbf{A}_{f2u1} & \mathbf{A}_{f2f2} & \mathbf{A}_{f2u0} & \mathbf{A}_{f2f0}\\ \hline \mathbf{A}_{u0u1} & \mathbf{A}_{u0f2} & \mathbf{A}_{u0u0} & \bar{\mathbf{A}}_{u0f0}\\ \mathbf{A}_{f0u1} & \mathbf{A}_{f0f2} & \bar{\mathbf{A}}_{f0u0} & \mathbf{A}_{f0f0}\end{array}\right| \left|\begin{array}{c}\mathbf{F}_1\\ -\mathbf{U}_2\\ \hline \mathbf{F}_0\\ -\mathbf{U}_0\end{array}\right| + \left|\begin{array}{c}\mathbf{A}_{u1\sigma}\\ \mathbf{A}_{f2\sigma}\\ \hline \mathbf{A}_{u0\sigma}\\ \mathbf{A}_{f0\sigma}\end{array}\right| \left|\ \mathbf{p}\ \right| + \beta \left|\begin{array}{c}\hat{\mathbf{W}}_1\\ \hat{\mathbf{P}}_2\\ \hline \hat{\mathbf{W}}_0\\ \hat{\mathbf{P}}_0\end{array}\right|. \tag{10}$$

In the latter block equation the matrix is symmetric. Moreover, the submatrices $\mathbf{A}$ and the subvectors $\mathbf{W}$, $\mathbf{P}$ are formed by coefficients obtained through a double integration according to the SGBEM strategy. In detail, the first and second rows represent the Dirichlet and Neumann conditions written in weighted form $\mathbf{W}_1 - \bar{\mathbf{W}}_1 = \mathbf{0}$ and $\mathbf{P}_2 - \bar{\mathbf{P}}_2 = \mathbf{0}$. The remaining rows regard the weighting of the displacements and tractions at the interface zones. The terms $\bar{\mathbf{A}}_{u0f0} = \bar{\mathbf{A}}_{f0u0}^T$ include the weighting of the CPV integrals and of the corresponding free terms.

The stress field (Eq. (9)) is obtained by the following equation:

$$|\boldsymbol{\sigma}| = \left|\mathbf{a}_{\sigma u1}\quad \mathbf{a}_{\sigma f2}\quad |\quad \mathbf{a}_{\sigma u0}\quad \mathbf{a}_{\sigma f0}\right| \left|\begin{array}{c}\mathbf{F}_1\\ -\mathbf{U}_2\\ \hline \mathbf{F}_0\\ -\mathbf{U}_0\end{array}\right| + |\mathbf{a}_{\sigma\sigma}||\mathbf{p}| + \beta|\hat{\mathbf{I}}_\sigma| \tag{11}$$

where the small letters are matrices containing coefficients obtained according to collocation BEM.

In order to analyze the plastic phenomenon, the domain is discretized by introducing several bem-elements in the zones where the plastic strains have to be stored during the load-unload process.

In Eq. (10) some coefficients show singular or hyper-singular kernels. These difficulties were overcome within the SGBEM approach by using different techniques. We can mention the strategies of Bonnet [31], Frangi and Novati [32], Panzeca et al. [15], Holzer [33] and Terravecchia [34].

In Eq. (11) the singularities regard the coefficients of the matrix $\mathbf{a}_{\sigma\sigma}$ located on the diagonal, the latter providing stress at the Gauss points due to plastic strain $\mathbf{p}$ distribution in the same bem-e. These integrals may be considered as Cauchy Principal Values with which the Bui free term [35] is associated. Otherwise, it is possible to employ the regularization technique with the aim of cutting off the strong singularity, followed by the Radial Integral Method (RIM) [25,36] in order to permit the transformation of the domain integrals into boundary ones. This strategy has to be used in each bem-e. The reader can refer to Panzeca et al. [17,37] and Zito et al. [20] for a more detailed discussion of the computational aspects and the related implementation techniques.

Eqs. (10) and (11) may be expressed in compact form in the following way:

$$\mathbf{0} = \mathbf{A}\mathbf{X} + \mathbf{A}_0\mathbf{X}_0 + \mathbf{A}_\sigma\mathbf{p} + \beta\,\hat{\mathbf{L}} \tag{12a}$$

$$\mathbf{Z}_0 = \mathbf{A}_0^T\mathbf{X} + \mathbf{A}_{00}\mathbf{X}_0 + \mathbf{A}_{0\sigma}\mathbf{p} + \beta\,\hat{\mathbf{L}}_0 \tag{12b}$$

$$\boldsymbol{\sigma} = \mathbf{a}_\sigma\mathbf{X} + \mathbf{a}_{\sigma 0}\mathbf{X}_0 + \mathbf{a}_{\sigma\sigma}\mathbf{p} + \beta\,\hat{\mathbf{I}}_\sigma \tag{12c}$$

where

$$\mathbf{Z}_0 = \begin{vmatrix} \mathbf{W}_0 \\ \mathbf{P}_0 \end{vmatrix}, \tag{13a}$$

$$\mathbf{X} = \begin{vmatrix} \mathbf{F}_1 \\ -\mathbf{U}_2 \end{vmatrix}, \tag{13b}$$

$$\mathbf{X}_0 = \begin{vmatrix} \mathbf{F}_0 \\ -\mathbf{U}_0 \end{vmatrix}, \tag{13c}$$

$$\hat{\mathbf{L}} = \begin{vmatrix} \hat{\mathbf{W}}_1 \\ \hat{\mathbf{P}}_2 \end{vmatrix}, \tag{13d}$$

$$\hat{\mathbf{L}}_0 = \begin{vmatrix} \hat{\mathbf{W}}_0 \\ \hat{\mathbf{P}}_0 \end{vmatrix}. \tag{13e}$$

The vector $\mathbf{Z}_0$ collects the generalized (or weighted) displacement $\mathbf{W}_0$ and traction $\mathbf{P}_0$ subvectors defined at the interface boundaries, obtained as the response to all the known and unknown actions, regarding the boundary and domain quantities. The vector $\boldsymbol{\sigma}$ represents the stresses, computed at the Gauss points, due to the same known and unknown actions.

By performing variable condensation through the replacement of the vector $\mathbf{X}$ extracted from Eq. (12a) into Eqs. (12b) and (12c), one obtains:

$$\mathbf{Z}_0 = \mathbf{D}_{00}\mathbf{X}_0 + \mathbf{D}_{0\sigma}\mathbf{p} + \beta\hat{\mathbf{Z}}_0 \tag{14a}$$

$$\boldsymbol{\sigma} = \mathbf{d}_{\sigma 0}\mathbf{X}_0 + \mathbf{d}_{\sigma\sigma}\mathbf{p} + \beta\hat{\boldsymbol{\sigma}} \tag{14b}$$

where one sets

$$\mathbf{D}_{00} = \mathbf{A}_0^T\mathbf{A}^{-1}\mathbf{A}_0 - \mathbf{A}_{00}, \tag{15a}$$

$$\mathbf{D}_{0\sigma} = -\mathbf{A}_0^T\mathbf{A}^{-1}\mathbf{A}_\sigma + \mathbf{A}_{0\sigma}, \tag{15b}$$

$$\hat{\mathbf{Z}}_0 = -\mathbf{A}_0^T\mathbf{A}^{-1}\hat{\mathbf{L}} + \hat{\mathbf{L}}_0, \tag{15c}$$

$$\mathbf{d}_{\sigma 0} = \mathbf{a}_\sigma\mathbf{A}^{-1}\mathbf{A}_0 - \mathbf{a}_{\sigma 0}, \tag{15d}$$

$$\mathbf{d}_{\sigma\sigma} = -\mathbf{a}_\sigma\mathbf{A}^{-1}\mathbf{a}_\sigma + \mathbf{a}_{\sigma\sigma}, \tag{15e}$$

$$\hat{\boldsymbol{\sigma}} = -\mathbf{a}_\sigma\mathbf{A}^{-1}\hat{\mathbf{L}} + \hat{\mathbf{I}}_\sigma. \tag{15f}$$

Eqs. (14a) and (14b) are two characteristic equations of each bem-e. They relate the generalized (or weighted) displacements and tractions $\mathbf{Z}_0$ defined on the interface zone Γ_0 and the stresses $\boldsymbol{\sigma}$ at the bem-e domain to the interface mechanical and kinematical nodal quantities $\mathbf{X}_0$, to the plastic strains $\mathbf{p}$ and to the load vectors $\hat{\mathbf{Z}}_0$ and $\hat{\boldsymbol{\sigma}}$. Moreover $\mathbf{D}_{00}$, $\mathbf{D}_{0\sigma}$, $\mathbf{d}_{\sigma 0}$, $\mathbf{d}_{\sigma\sigma}$ are appropriate stiffness matrices of the bem-e.

2.2. Bem-element assembling

We start by subdividing the body into m bem-e and in considering for each of these elements Eqs. (14a) and (14b). Thus we obtain two global relations related to all the bem-elements considered, i.e.:

$$\begin{vmatrix} \mathbf{Z}_0^1 \\ \vdots \\ \mathbf{Z}_0^m \end{vmatrix} = \begin{vmatrix} \mathbf{D}_{00}^1 & \dots & \mathbf{0} \\ \vdots & \ddots & \vdots \\ \mathbf{0} & \dots & \mathbf{D}_{00}^m \end{vmatrix} \begin{vmatrix} \mathbf{X}_0^1 \\ \vdots \\ \mathbf{X}_0^m \end{vmatrix} + \begin{vmatrix} \mathbf{D}_{0\sigma}^1 & \dots & \mathbf{0} \\ \vdots & \ddots & \vdots \\ \mathbf{0} & \dots & \mathbf{D}_{0\sigma}^m \end{vmatrix} \begin{vmatrix} \mathbf{p}^1 \\ \vdots \\ \mathbf{p}^m \end{vmatrix} + \beta \begin{vmatrix} \hat{\mathbf{Z}}_0^1 \\ \vdots \\ \hat{\mathbf{Z}}_0^m \end{vmatrix} \tag{16a}$$

$$\begin{vmatrix} \boldsymbol{\sigma}^1 \\ \vdots \\ \boldsymbol{\sigma}^m \end{vmatrix} = \begin{vmatrix} \mathbf{d}_{\sigma 0}^1 & \dots & \mathbf{0} \\ \vdots & \ddots & \vdots \\ \mathbf{0} & \dots & \mathbf{d}_{\sigma 0}^m \end{vmatrix} \begin{vmatrix} \mathbf{X}_0^1 \\ \vdots \\ \mathbf{X}_0^m \end{vmatrix} + \begin{vmatrix} \mathbf{d}_{\sigma\sigma}^1 & \dots & \mathbf{0} \\ \vdots & \ddots & \vdots \\ \mathbf{0} & \dots & \mathbf{d}_{\sigma\sigma}^m \end{vmatrix} \begin{vmatrix} \mathbf{p}^1 \\ \vdots \\ \mathbf{p}^m \end{vmatrix} + \beta \begin{vmatrix} \hat{\boldsymbol{\sigma}}^1 \\ \vdots \\ \hat{\boldsymbol{\sigma}}^m \end{vmatrix} \tag{16b}$$

or in compact form

$$\mathbf{Z}_0 = \mathbf{D}_{00}\mathbf{X}_0 + \mathbf{D}_{0\sigma}\mathbf{p} + \beta\hat{\mathbf{Z}}_0 \tag{17a}$$

$$\boldsymbol{\sigma} = \mathbf{d}_{\sigma 0}\mathbf{X}_0 + \mathbf{d}_{\sigma\sigma}\mathbf{p} + \beta\hat{\boldsymbol{\sigma}} \tag{17b}$$

formally equal to Eqs. (14a) and (14b), but regarding all the bem-elements in a global form.

We introduce the nodal interface vector $\boldsymbol{\zeta}_0$ of the mechanical and kinematical unknowns related to the assembled system and perform a suitable nodal variable condensation through the matrices of equilibrium $\mathbf{L}^T$ and of compatibility $\mathbf{N}$, respectively:

$$\left|\begin{array}{c} \mathbf{F}_0^1 \\ -\mathbf{U}_0^1 \\ \hline \dots \\ \dots \\ \hline \mathbf{F}_0^m \\ -\mathbf{U}_0^m \end{array}\right| = \left|\begin{array}{cc} (\mathbf{L}^1)^T & \mathbf{0} \\ \mathbf{0} & \mathbf{N}^1 \\ \hline \dots & \dots \\ \dots & \dots \\ \hline (\mathbf{L}^m)^T & \mathbf{0} \\ \mathbf{0} & \mathbf{N}^m \end{array}\right| \left|\begin{array}{c} \mathbf{F}_0 \\ -\mathbf{U}_0 \end{array}\right| \quad i.e. \quad \mathbf{X}_0 = \mathbf{E}\,\zeta_0. \tag{18}$$

The latter relation has to be considered as a strong regularity condition.

The same transposed matrices $\mathbf{L}$ and $\mathbf{N}^T$ define the weighted equilibrium and compatibility, respectively.

$$\left|\begin{array}{cc} \mathbf{L}^1 & \mathbf{0} \\ \mathbf{0} & (\mathbf{N}^1)^T \end{array}\right| \left|\begin{array}{cc} \dots & \dots \\ \dots & \dots \end{array}\right| \left|\begin{array}{cc} \mathbf{L}^m & \mathbf{0} \\ \mathbf{0} & (\mathbf{N}^m)^T \end{array}\right| \left|\begin{array}{c} \mathbf{W}_0^1 \\ \mathbf{P}_0^1 \\ \hline \dots \\ \dots \\ \hline \mathbf{W}_0^m \\ \mathbf{P}_0^m \end{array}\right| = \left|\begin{array}{c} \mathbf{0} \\ \mathbf{0} \end{array}\right| \quad i.e. \quad \mathbf{E}^T\,\mathbf{Z}_0 = \mathbf{0}. \tag{19}$$

The latter relation has to be considered as a weak regularity condition.

Eqs. (18) and (19) introduced in Eqs. (17a) and (17b) give rise to the following relations:

$$\mathbf{K}_{00}\boldsymbol{\zeta}_0 + \mathbf{K}_{0\sigma}\mathbf{p} + \beta\hat{\mathbf{f}}_0 = \mathbf{0} \tag{20a}$$

$$\boldsymbol{\sigma} = \mathbf{k}_{\sigma 0}\boldsymbol{\zeta}_0 + \mathbf{k}_{\sigma\sigma}\mathbf{p} + \beta\hat{\boldsymbol{\sigma}} \tag{20b}$$

where the following positions are valid:

$$\mathbf{K}_{00} = \mathbf{E}^T\mathbf{D}_{00}\mathbf{E}, \qquad \mathbf{K}_{0\sigma} = \mathbf{E}^T\mathbf{D}_{0\sigma}, \qquad \hat{\mathbf{f}}_0 = \mathbf{E}^T\hat{\mathbf{Z}}_0, \qquad \mathbf{k}_{\sigma 0} = \mathbf{d}_{\sigma 0}\mathbf{E}, \qquad \mathbf{k}_{\sigma\sigma} = \mathbf{d}_{\sigma\sigma}. \tag{21}$$

Introducing a new variable condensation through the replacement of the $\boldsymbol{\zeta}_0$ vector extracted from Eq. (20a) into Eq. (20b), the self-equilibrium stress equation is obtained:

$$\boldsymbol{\sigma} = \mathbf{K}\mathbf{p} + \beta\hat{\boldsymbol{\sigma}}_s \tag{22}$$

where

$$\mathbf{K} = -\mathbf{k}_{\sigma 0}\mathbf{K}_{00}^{-1}\mathbf{K}_{0\sigma} + \mathbf{k}_{\sigma\sigma}, \tag{23a}$$

$$\hat{\boldsymbol{\sigma}}_s = -\mathbf{k}_{\sigma 0}\mathbf{K}_{00}^{-1}\hat{\mathbf{f}}_0 + \hat{\boldsymbol{\sigma}}. \tag{23b}$$

Eq. (22) provides the stress at the Gauss points of each bem-e as a function of the plastic strains $\mathbf{p}$ and of the external actions $\hat{\boldsymbol{\sigma}}_s$, the latter amplified by β. $\mathbf{K}$ is defined as a self-stress influence matrix, fully-populated, not symmetric and semi-defined negative [21]. The evaluation of this matrix only involves the elastic characteristic of the material and the structure geometry.

3. Constitutive relations for rate-independent plasticity and the return mapping algorithm

The governing equations of classical plasticity will now be briefly summarized.

The stress vector is related to the elastic strain ($\boldsymbol{\varepsilon} - \boldsymbol{\varepsilon}^p$) through the standard elasticity tensor $\mathbf{D}$, i.e.

$$\boldsymbol{\sigma} = \mathbf{D}\,(\boldsymbol{\varepsilon} - \boldsymbol{\varepsilon}^p) \tag{24}$$

The essential feature that characterizes the plastic constitutive law is that the stress solution must belong to the space of the admissible stresses:

$$F[\boldsymbol{\sigma}, \boldsymbol{\rho}] \leq 0. \tag{25}$$

F being the yield function and $\boldsymbol{\rho}$ the internal variable (back-stress) vector which define the kinematical part of the hardening behaviour.

The irreversible part of the plastic process is given by the evolution of the plastic strain $\dot{\boldsymbol{\varepsilon}}^p$ and of the back-stress $\dot{\boldsymbol{\rho}}$. The evolution laws, called *flow rule* and *hardening law,* are defined by the following incremental laws:

$$\dot{\boldsymbol{\varepsilon}}^p = \dot{\lambda}\partial_{\boldsymbol{\sigma}} F[\boldsymbol{\sigma}, \boldsymbol{\rho}], \tag{26a}$$

$$\dot{\boldsymbol{\rho}} = \dot{\lambda}\mathbf{H}\partial_{\boldsymbol{\rho}} F[\boldsymbol{\sigma}, \boldsymbol{\rho}] \tag{26b}$$

where $\dot{\lambda}$ is the increment in the plastic multiplier and is defined by means of the following loading/unloading conditions:

$$\dot{\lambda} \geq 0, \tag{27a}$$

$$F[\boldsymbol{\sigma}, \boldsymbol{\rho}] \leq 0, \tag{27b}$$

$$\dot{\lambda} F[\boldsymbol{\sigma}, \boldsymbol{\rho}] = 0. \tag{27c}$$

Let us consider the classical theory developed by Simo and Hughes [38], called operator split, where the implicit–backward Euler scheme is applied to Eqs. (26). The following equations, governing the elastoplastic analysis, can be obtained for the elastic predictor:

$$\boldsymbol{\sigma}^*_{n+1} = \boldsymbol{\sigma}_n + \Delta\boldsymbol{\sigma}_{n+1} \tag{28}$$

and for the plastic corrector:

$$\begin{cases} \boldsymbol{\sigma}_{n+1} = \boldsymbol{\sigma}^*_{n+1} - \Delta\lambda_{n+1}\mathbf{D}\partial_{\boldsymbol{\sigma}_{n+1}} F[\boldsymbol{\sigma}_{n+1}, \boldsymbol{\rho}_{n+1}] & \text{(a)} \\ \boldsymbol{\rho}_{n+1} = \boldsymbol{\rho}_n + \Delta\lambda_{n+1}\mathbf{H}\partial_{\boldsymbol{\rho}_{n+1}} F[\boldsymbol{\sigma}_{n+1}, \boldsymbol{\rho}_{n+1}] & \text{(b)} \\ F[\boldsymbol{\sigma}_{n+1}, \boldsymbol{\rho}_{n+1}] = 0 & \text{(c)} \end{cases} \tag{29}$$

$\mathbf{H}$ being the matrix of the hardening moduli and $\Delta\lambda$ the plastic multiplier increment.

It is important to note that the same result can be obtained through the extremal path theory [39,40] or by the closest point return mapping algorithm [38].

The indices n and $n+1$ represent the previous and the current load step, and $\boldsymbol{\sigma}^*$ the elastic (trial) stress. In the hypothesis of a plane strain state, Eq. (29) represents a nonlinear equation system in the unknowns $\boldsymbol{\sigma}_{n+1}$, $\boldsymbol{\rho}_{n+1}$, $\Delta\lambda_{n+1}$.

In particular, with regard to the case of a 2D continuous solid and in the hypothesis of a plane strain condition, associated plastic flow rule, linear kinematic hardening and von Mises yield law, Eqs. (29) can be rewritten in the following form:

$$\begin{cases} \boldsymbol{\sigma}_{n+1} - \boldsymbol{\sigma}^*_{n+1} + \Delta\lambda_{n+1}\mathbf{D}\boldsymbol{M}(\boldsymbol{\sigma}_{n+1} - \boldsymbol{\rho}_{n+1}) = \mathbf{0} & \text{(a)} \\ \boldsymbol{\rho}_{n+1} - \boldsymbol{\rho}_n - \Delta\lambda_{n+1}\mathbf{H}\boldsymbol{M}(\boldsymbol{\sigma}_{n+1} - \boldsymbol{\rho}_{n+1}) = \mathbf{0} & \text{(b)} \\ \dfrac{1}{2}(\boldsymbol{\sigma}_{n+1} - \boldsymbol{\rho}_{n+1})^T\boldsymbol{M}(\boldsymbol{\sigma}_{n+1} - \boldsymbol{\rho}_{n+1}) - \sigma_y^2 = 0 & \text{(c)} \end{cases} \tag{30}$$

σ_y being the yield stress and $\boldsymbol{M}$ a matrix of constants [40].

The unknowns $\boldsymbol{\sigma}_{n+1}$, $\boldsymbol{\rho}_{n+1}$ and $\Delta\lambda_{n+1}$ of this nonlinear problem may be obtained by applying the standard or modified N–R procedures.

4. The elastoplastic algorithm for active macro-zones

In the elastoplastic analysis a return mapping algorithm has to be performed through the N–R procedure considering all the plastically active macro-zones.

This approach utilizes the self-equilibrium stress equation to compute the trial stresses in the predictor phase and uses the self-stress matrix coefficients, changed in sign, to perform the corrector phase, the latter considered as a discrete nonlocal strategy.

Elastic predictor phase

Let us start to compute the trial stresses, i.e. the purely elastic response at the instant $n + 1$ in each bem-element of the discretized body.

For this purpose, Eq. (22) provides the predictors $\boldsymbol{\sigma}^*_{(n+1)}$ as a function of the stored plastic strains $\mathbf{p}_{(n+1)} = \mathbf{p}_{(n)} + \Delta\mathbf{p}$, imposed as volumetric distortions, and of the load increment $\beta_{(n+1)} = \beta_{(n)} + \Delta\beta$:

$$\boldsymbol{\sigma}^*_{(n+1)} = \mathbf{K}\left(\mathbf{p}_{(n)} + \Delta\mathbf{p}\right) + \beta_{(n+1)}\,\hat{\boldsymbol{\sigma}}_s \tag{31}$$

where $\Delta\mathbf{p}$ is the plastic strain increment vector evaluated by the corrector phase inside the $n+1$ load step and $\mathbf{K}$ is the self-stress influence matrix, fully-populated, and regards all the m bem-elements.

It is necessary to check the plastic consistency condition at the Gauss points of all the m bem-elements by using the von Mises yield law, where the elastic domain is moved by $\boldsymbol{\rho}_{i(n+1)}$ during the loading/unloading process:

$$F[\boldsymbol{\sigma}^*_{i(n+1)}, \boldsymbol{\rho}_{i(n+1)}] = \frac{1}{2}(\boldsymbol{\sigma}^*_{i(n+1)} - \boldsymbol{\rho}_{i(n+1)})^T \boldsymbol{M}(\boldsymbol{\sigma}^*_{i(n+1)} - \boldsymbol{\rho}_{i(n+1)}) - \sigma^2_{iy} \le 0 \tag{32}$$

$i = 1, \ldots, m$ being the generic bem-e.

In the active $a \le m$ bem-elements where the inequality (32) is violated, i.e. $F[\boldsymbol{\sigma}^*_{i(n+1)}, \boldsymbol{\rho}_{i(n+1)}] > 0$, a corrector phase occurs, involving the birth of self-stresses and of the internal variables caused by the plastic strains.

Plastic corrector phase

The corrector phase uses the first term of Eq. (22), i.e. $\boldsymbol{\sigma}^p = \mathbf{K}\,\Delta\mathbf{p}$, to obtain the elastoplastic solution in every bem-e where the plastic consistency condition appears to be violated. In this phase the vectors $\boldsymbol{\sigma}$, $\boldsymbol{\rho}$ and the scalar $\Delta\lambda$ are unknowns, whereas the vector $\Delta\mathbf{p} = \mathbf{f}[\Delta\lambda, \boldsymbol{\sigma}, \boldsymbol{\rho}]$ is the volumetric plastic strain to impose for every plastically active bem-e of the discretized body, in order to have a plastically admissible stress field.

To reach this goal a strategy, called active macro-zone analysis, may be employed. It permits one to obtain the solution by a global nonlinear equation system involving all the active bem-elements through simultaneous satisfaction of the plastic consistency conditions. This strategy shows the remarkable advantage of using a low number of plastic loops and the drawback of working with Jacobian operators usually having large dimensions.

In a similar way to what is shown in Section 3, Eq. (29) is written for a discrete system having a active bem-elements. The corrector phase is applied simultaneously to the active macro-zones identified in the previous predictor phase through the following equations:

$$\begin{cases} \boldsymbol{\sigma}_{A(n+1)} = \boldsymbol{\sigma}^*_{A(n+1)} - \boldsymbol{\sigma}^p_{A(n+1)} & \text{(a)} \\ \boldsymbol{\rho}_{A(n+1)} = \boldsymbol{\rho}_{A(n)} + \boldsymbol{\rho}^p_{A(n+1)} & \text{(b)} \\ \mathbf{F}_A[\boldsymbol{\sigma}_{A(n+1)}, \boldsymbol{\rho}_{A(n+1)}] = \mathbf{0} & \text{(c)} \end{cases} \tag{33}$$

where $\boldsymbol{\sigma}^p_{A(n+1)} = \mathbf{K}_{AA}\Delta\mathbf{p}_{A(n+1)}$ represents the nonlocal self-stress vector which replaces the local $\mathbf{D}\,\Delta\boldsymbol{\varepsilon}^p_{n+1}$ contribution of Eq. (29)(a) and $\boldsymbol{\rho}^p_{A(n+1)}$ preserves the local characteristic.

For simplicity, in the next equations the $n+1$ subindex will be omitted and $\boldsymbol{\rho}_{(n)} = \tilde{\boldsymbol{\rho}}$ will be assumed.

In the hypothesis that the shape function defined in Eq. (7g) is the same as the shape function related to the plastic multiplier increment, i.e. $\Delta\lambda_h = \boldsymbol{\psi}_p \Delta\Lambda_h$ with $\boldsymbol{\psi}_p \ge 0$, the plastic flow and hardening law vectors, related to all the active bem-elements, can be expressed as:

$$\Delta\mathbf{p}_A = \begin{vmatrix} \Delta\mathbf{p}_1 \\ \vdots \\ \Delta\mathbf{p}_a \end{vmatrix} = \begin{vmatrix} \Delta\Lambda_1 \partial_{\boldsymbol{\sigma}_1} F[\boldsymbol{\sigma}_1, \boldsymbol{\rho}_1] \\ \vdots \\ \Delta\Lambda_a\, \partial_{\boldsymbol{\sigma}_a} F[\boldsymbol{\sigma}_a, \boldsymbol{\rho}_a] \end{vmatrix} = \begin{vmatrix} \Delta\Lambda_1 \boldsymbol{M}(\boldsymbol{\sigma}_1 - \boldsymbol{\rho}_1) \\ \vdots \\ \Delta\Lambda_a \boldsymbol{M}(\boldsymbol{\sigma}_a - \boldsymbol{\rho}_a) \end{vmatrix} \tag{34a}$$

$$\boldsymbol{\rho}^p_A = \begin{vmatrix} \boldsymbol{\rho}_1 \\ \vdots \\ \boldsymbol{\rho}_a \end{vmatrix} = \begin{vmatrix} \Delta\Lambda_1\, \mathbf{H}_1\, \partial_{\boldsymbol{\rho}_1} F[\boldsymbol{\sigma}_1, \boldsymbol{\rho}_1] \\ \vdots \\ \Delta\Lambda_a\, \mathbf{H}_a\, \partial_{\boldsymbol{\rho}_a} F[\boldsymbol{\sigma}_a, \boldsymbol{\rho}_a] \end{vmatrix} = \begin{vmatrix} \Delta\Lambda_1 \mathbf{H}_1 \boldsymbol{M}(\boldsymbol{\sigma}_1 - \boldsymbol{\rho}_1) \\ \vdots \\ \Delta\Lambda_a \mathbf{H}_a \boldsymbol{M}(\boldsymbol{\sigma}_a - \boldsymbol{\rho}_a) \end{vmatrix}. \tag{34b}$$

As a consequence, the nonlinear system (33) can also be rewritten in the following form:

$$\begin{cases} \mathbf{F}_\sigma \equiv \boldsymbol{\sigma}_A - \boldsymbol{\sigma}^*_A + \mathbf{K}_{AA}\Delta\mathbf{p}_A = \mathbf{0} & \text{(a)} \\ \mathbf{F}_\rho \equiv \boldsymbol{\rho}_A - \tilde{\boldsymbol{\rho}}_A - \boldsymbol{\rho}^p_A = \mathbf{0} & \text{(b)} \\ \mathbf{F}_\Lambda \equiv \mathbf{F}_A[\boldsymbol{\sigma}_A, \boldsymbol{\rho}_A] = \mathbf{0} & \text{(c)} \end{cases} \tag{35}$$

where one assumes:

$$\boldsymbol{\sigma}_A = \begin{vmatrix} \boldsymbol{\sigma}_1 \\ \vdots \\ \boldsymbol{\sigma}_a \end{vmatrix}, \qquad \boldsymbol{\sigma}^*_A = \begin{vmatrix} \boldsymbol{\sigma}^*_1 \\ \vdots \\ \boldsymbol{\sigma}^*_a \end{vmatrix}, \qquad \mathbf{K}_{AA} = \begin{vmatrix} -\mathbf{K}_{11} & \cdots & -\mathbf{K}_{1a} \\ \vdots & \ddots & \vdots \\ -\mathbf{K}_{a1} & \cdots & -\mathbf{K}_{aa} \end{vmatrix},$$

$$\boldsymbol{\rho}_A = \begin{vmatrix} \boldsymbol{\rho}_1 \\ \vdots \\ \boldsymbol{\rho}_a \end{vmatrix}, \qquad \tilde{\boldsymbol{\rho}}_A = \begin{vmatrix} \tilde{\boldsymbol{\rho}}_1 \\ \vdots \\ \tilde{\boldsymbol{\rho}}_a \end{vmatrix}, \qquad \mathbf{F}_A[\boldsymbol{\sigma}_A, \boldsymbol{\rho}_A] = \begin{vmatrix} \frac{1}{2}(\boldsymbol{\sigma}_1 - \boldsymbol{\rho}_1)^T \boldsymbol{M}(\boldsymbol{\sigma}_1 - \boldsymbol{\rho}_1) - \sigma^2_{1y} \\ \vdots \\ \frac{1}{2}(\boldsymbol{\sigma}_a - \boldsymbol{\rho}_a)^T \boldsymbol{M}(\boldsymbol{\sigma}_a - \boldsymbol{\rho}_a) - \sigma^2_{ay} \end{vmatrix}. \tag{36}$$

The $\mathbf{K}_{AA}$ matrix is positive semi-definite and derives from the $\mathbf{K}$ matrix present in Eq. (22), extracting the blocks relative to the a plastically active bem-elements, changed in sign.

In the first function $\mathbf{F}_\sigma$, $\boldsymbol{\sigma}_A$ is the total stress vector, $\boldsymbol{\sigma}_A^*$ the trial stress, and $\mathbf{K}_{AA}\Delta\mathbf{p}_A$ the corrective self-stress vector containing the local and nonlocal contributions. The functions $\mathbf{F}_\rho$ and $\mathbf{F}_\Lambda$ only have local contributions.

Eq. (35) is a nonlinear equation system in the unknowns: stresses $\boldsymbol{\sigma}_A$, back-stresses $\boldsymbol{\rho}_A$ and plastic multipliers $\Delta\boldsymbol{\Lambda}_A$ for the active macro-zone bem-elements.

The approximate solution of this nonlinear problem is here obtained by applying the standard N–R procedure:

$$\left|\begin{array}{c|c|c} \mathbf{J}^j_{\sigma\sigma} & \mathbf{J}^j_{\sigma\rho} & \mathbf{J}^j_{\sigma\Lambda} \\ \hline \mathbf{J}^j_{\rho\sigma} & \mathbf{J}^j_{\rho\rho} & \mathbf{J}^j_{\rho\Lambda} \\ \mathbf{J}^j_{\Lambda\sigma} & \mathbf{J}^j_{\Lambda\rho} & \mathbf{J}^j_{\Lambda\Lambda} \end{array}\right| \left|\begin{array}{c} \boldsymbol{\sigma}_A^{j+1} - \boldsymbol{\sigma}_A^j \\ \hline \boldsymbol{\rho}_A^{j+1} - \boldsymbol{\rho}_A^j \\ \Delta\Lambda_A^{j+1} - \Delta\Lambda_A^j \end{array}\right| = \left|\begin{array}{c} -\mathbf{F}^j_\sigma \\ \hline -\mathbf{F}^j_\rho \\ -\mathbf{F}^j_\Lambda \end{array}\right| \tag{37}$$

or in compact form:

$$\mathbf{J}^j_{AA}\left(\mathbf{Y}_A^{j+1} - \mathbf{Y}_A^j\right) = -\mathbf{F}^j_A \tag{38}$$

where the apex j is related to the N–R recursive procedure.

The generic block $\mathbf{J}^j_{\alpha\delta} = [\partial_\delta \mathbf{F}_\alpha]^j$ of the Jacobian matrix $\mathbf{J}^j_{AA}$, represents the derivate of function $\mathbf{F}_\alpha$ (with $\alpha = \sigma,\ \rho,\ \Lambda$) with respect to the variable δ (with $\boldsymbol{\delta} = \boldsymbol{\sigma}_A, \boldsymbol{\rho}_A, \Delta\boldsymbol{\Lambda}_A$).

The Jacobian operator $\mathbf{J}^j_{AA}$ is non-symmetric and collects the submatrices $\mathbf{J}^j_{\rho\sigma}, \mathbf{J}^j_{\rho\rho}, \mathbf{J}^j_{\rho\Lambda}, \mathbf{J}^j_{\Lambda\sigma}$ and $\mathbf{J}^j_{\Lambda\rho}$ having diagonal blocks, and the submatrix $\mathbf{J}^j_{\Lambda\Lambda}$ which is null.

The vector $\mathbf{Y}_A^{j+1}$ is the approximate solution in terms of stresses, internal variables and plastic multipliers evaluated at the Gauss points of the plastically active macro-zone bem-elements.

The use of the self-stress $\mathbf{K}_{AA}$ matrix means that this procedure may provide the nonlocal solution in the plastically active macro-zones, where the plastic consistency conditions prove to be satisfied simultaneously.

5. Computational burden reduction in the N–R procedure

The Jacobian operator $\mathbf{J}^j_{AA}$ is usually of large dimensions, and therefore the updating and inversion of this operator may prove onerous.

We introduce a strategy that has the aim of reducing the computational efforts due to the updating and subsequent inversion of this operator in the recursive process.

The nonlinear system of equation (37) may be rewritten in the following form:

$$\left|\begin{array}{c|c} \mathbf{J}^j_{\sigma\sigma} & \mathbf{J}^j_{\sigma r} \\ \hline \mathbf{J}^j_{r\sigma} & \mathbf{J}^j_{rr} \end{array}\right| \left|\begin{array}{c} \boldsymbol{\sigma}_A^{j+1} - \boldsymbol{\sigma}_A^j \\ \hline \mathbf{r}_A^{j+1} - \mathbf{r}_A^j \end{array}\right| = \left|\begin{array}{c} -\mathbf{F}^j_\sigma \\ \hline -\mathbf{F}^j_r \end{array}\right| \tag{39}$$

where one assumes

$$\mathbf{J}^j_{\sigma r} = \left|\mathbf{J}^j_{\sigma\rho} \quad \mathbf{J}^j_{\sigma\Lambda}\right|, \tag{40a}$$

$$\mathbf{J}^j_{r\sigma} = \left|\begin{array}{c} \mathbf{J}^j_{\rho\sigma} \\ \mathbf{J}^j_{\Lambda\sigma} \end{array}\right|, \tag{40b}$$

$$\mathbf{J}^j_{rr} = \left|\begin{array}{cc} \mathbf{J}^j_{\rho\rho} & \mathbf{J}^j_{\rho\Lambda} \\ \mathbf{J}^j_{\Lambda\rho} & \mathbf{J}^j_{\Lambda\Lambda} \end{array}\right|, \tag{40c}$$

$$\mathbf{r}_A^{j+1} - \mathbf{r}_A^j = \left|\begin{array}{c} \boldsymbol{\rho}_A^{j+1} - \boldsymbol{\rho}_A^j \\ \Delta\boldsymbol{\Lambda}_A^{j+1} - \Delta\boldsymbol{\Lambda}_A^j \end{array}\right|, \tag{40d}$$

$$\mathbf{F}^j_r = \left|\begin{array}{c} \mathbf{F}^j_\rho \\ \mathbf{F}^j_\Lambda \end{array}\right| \tag{40e}$$

or in explicit form

$$\begin{cases} \mathbf{J}^j_{\sigma\sigma}\left(\boldsymbol{\sigma}_A^{j+1} - \boldsymbol{\sigma}_A^j\right) + \mathbf{J}^j_{\sigma r}\left(\mathbf{r}_A^{j+1} - \mathbf{r}_A^j\right) = -\mathbf{F}^j_\sigma & \text{(a)} \\ \mathbf{J}^j_{r\sigma}\left(\boldsymbol{\sigma}_A^{j+1} - \boldsymbol{\sigma}_A^j\right) + \mathbf{J}^j_{rr}\left(\mathbf{r}_A^{j+1} - \mathbf{r}_A^j\right) = -\mathbf{F}^j_r & \text{(b)} \end{cases} \tag{41}$$

with obvious meaning of symbols.

By performing a diagonalization process of Eqs. (41), one obtains:

$$\left|\begin{array}{c|c} \mathbf{J}^j_{ss} & \mathbf{0} \\ \hline \mathbf{0} & \mathbf{J}^j_{rr} \end{array}\right| \left|\begin{array}{c} \boldsymbol{\sigma}^{j+1}_A - \boldsymbol{\sigma}^j_A \\ \hline \mathbf{r}^{j+1}_A - \mathbf{r}^j_A \end{array}\right| = \left|\begin{array}{c} -\mathbf{F}^j_S \\ \hline -\mathbf{F}^j_R \end{array}\right| \tag{42}$$

where

$$\mathbf{J}^j_{ss} = \mathbf{J}^j_{\sigma\sigma} - \mathbf{J}^j_{\sigma r}(\mathbf{J}^j_{rr})^{-1}\mathbf{J}^j_{r\sigma}, \qquad \mathbf{F}^j_S = \mathbf{J}^j_{r\sigma}(\mathbf{J}^j_{rr})^{-1}\mathbf{F}^j_r - \mathbf{F}^j_\sigma, \qquad \mathbf{F}^j_R = \mathbf{J}^j_{r\sigma}(\mathbf{J}^j_{ss})^{-1}\mathbf{F}^j_S - \mathbf{F}^j_r. \tag{43}$$

The solution of Eq. (42) proves more advantageous, in comparison with Eq. (37), since the two equations are de-coupled and the inversion only concerns two blocks, that is $\mathbf{J}^j_{ss}$ and $\mathbf{J}^j_{rr}$. In detail the submatrix $\mathbf{J}^j_{ss}$ has small dimensions, while the submatrix $\mathbf{J}^j_{rr}$ is formed by diagonal blocks. As a consequence it is easy to prove that its inverse

$$\mathbf{J}^{-1}_{rr} = \left|\begin{array}{c|c} \mathbf{J}^{-1}_{\rho\rho} - \mathbf{J}^{-1}_{\rho\rho}\mathbf{J}_{\rho\Lambda}\mathbf{G}^{-1}_{\Lambda\Lambda}\mathbf{J}_{\Lambda\rho}\mathbf{J}^{-1}_{\rho\rho} & \mathbf{J}^{-1}_{\rho\rho}\mathbf{J}_{\rho\Lambda}\mathbf{G}^{-1}_{\Lambda\Lambda} \\ \hline \mathbf{G}^{-1}_{\Lambda\Lambda}\mathbf{J}_{\Lambda\rho}\mathbf{J}^{-1}_{\rho\rho} & -\mathbf{G}^{-1}_{\Lambda\Lambda} \end{array}\right| \quad \text{with } \mathbf{G}_{\Lambda\Lambda} = \mathbf{J}_{\Lambda\rho}\mathbf{J}^{-1}_{\rho\rho}\mathbf{J}_{\rho\Lambda} \tag{44}$$

is easily invertible with lower CPU times than Eq. (37).

Subsequently, from the solution vector $\mathbf{Y}^{j+1}_A$ it is possible to obtain the plastic strain increment vector $\Delta\mathbf{p}_A$ and the new back-stress vector $\boldsymbol{\rho}_A$ associated with the load step $n+1$ and related to the active bem-elements only. These vectors allow one to update the global vectors for the purpose of computing the new trial stress and verifying the plastic consistency condition of the yield domains in a restricted iterative process.

In Fig. 1 the elastoplastic procedure is shown. It is important to note that the updating of the nodal solution $\boldsymbol{\zeta}_{0(n+1)}$ and $\mathbf{X}_{(n+1)}$ is performed at the end of the $n+1$ load increment, contrary to what happens in other formulations, which need continuous correction of the nodal solution for each plastic iteration.

6. Numerical results

In order to show the efficiency of the proposed method some numerical tests were performed under the following hypotheses: plane strain condition, perfect plasticity or kinematic hardening, von Mises law and associated plastic flow rule.

These applications prove the good performance of the proposed strategy, implemented as an additional module inside Karnak.sGbem code [30]. The advantage lies in a better response, because it is based on

- the symmetric BEM where the fundamental solutions are used in every bem-element into which the body is subdivided. Indeed the compatibility and equilibrium are guaranteed at any point in each domain;
- the use of the mixed boundary value approach of the symmetric BEM where the boundary conditions regarding the compatibility and the equilibrium are introduced in both strong and weak form (see Panzeca and Salerno, [13]);
- the transfer of the domain inelastic actions into the boundary action in closed form [17,21,25,36,37];
- the updating of the plastic strains in the bem-elements which define the active macro-zones in a nonlocal strategy;
- a strategy which reduces the computational efforts of the Jacobian operator inversion in the N–R recursive process;
- the location of the elastic macroelements, only involving the boundary unknowns with strong variable reduction.

From the computational point of view, all the coefficients of the elastic matrices are computed in closed form. The symmetric matrices, definite in sign obtained, are naturally ill-conditioned, but the adopted matrix inversion technique, based on the Gauss method, used a particular pivot strategy.

6.1. Cube subjected to imposed displacement

In this first example, the response of a cube (Fig. 2) subjected to uniaxial imposed tensile displacement is evaluated. The material characteristics are: Young's modulus $E = 1$ MPa and Poisson's ratio $\nu = 0.3$, whereas the uniaxial yield value is $\sigma_y = 0,8$ MPa. Further, tolerance $Tol = 0.001$ was chosen in the return mapping analysis.

This example is intended to illustrate the perfect plasticity, the kinematical hardening and the softening phenomena under monotonically increasing uniaxial imposed displacements. The material satisfies the von Mises criterion.

The cube is discretized by 49 linear bem-elements and the "roller" condition is imposed at the two planes $x = 0$, $y = 0$. The computation is made with controlled displacements and the results shown in Fig. 3a, b, c are representative of the vertical stresses σ_y, at the bem-e marked by A, for the perfect plasticity ($H = 0$), hardening ($H = 0.1$), and softening ($H = -0.1$) cases, respectively.

It can be observed that the results calculated by the present method are in excellent agreement with the Gao and Davies solution [36].

6.2. Plate with circular hole

In the present subsection a thin square plate with a circular hole (Fig. 4a), subjected to uniform tensile load $q = 100$ MPa, is considered. The internal discretization is made by 144 bem-elements (Fig. 4b) and is characterized by linear modelling of

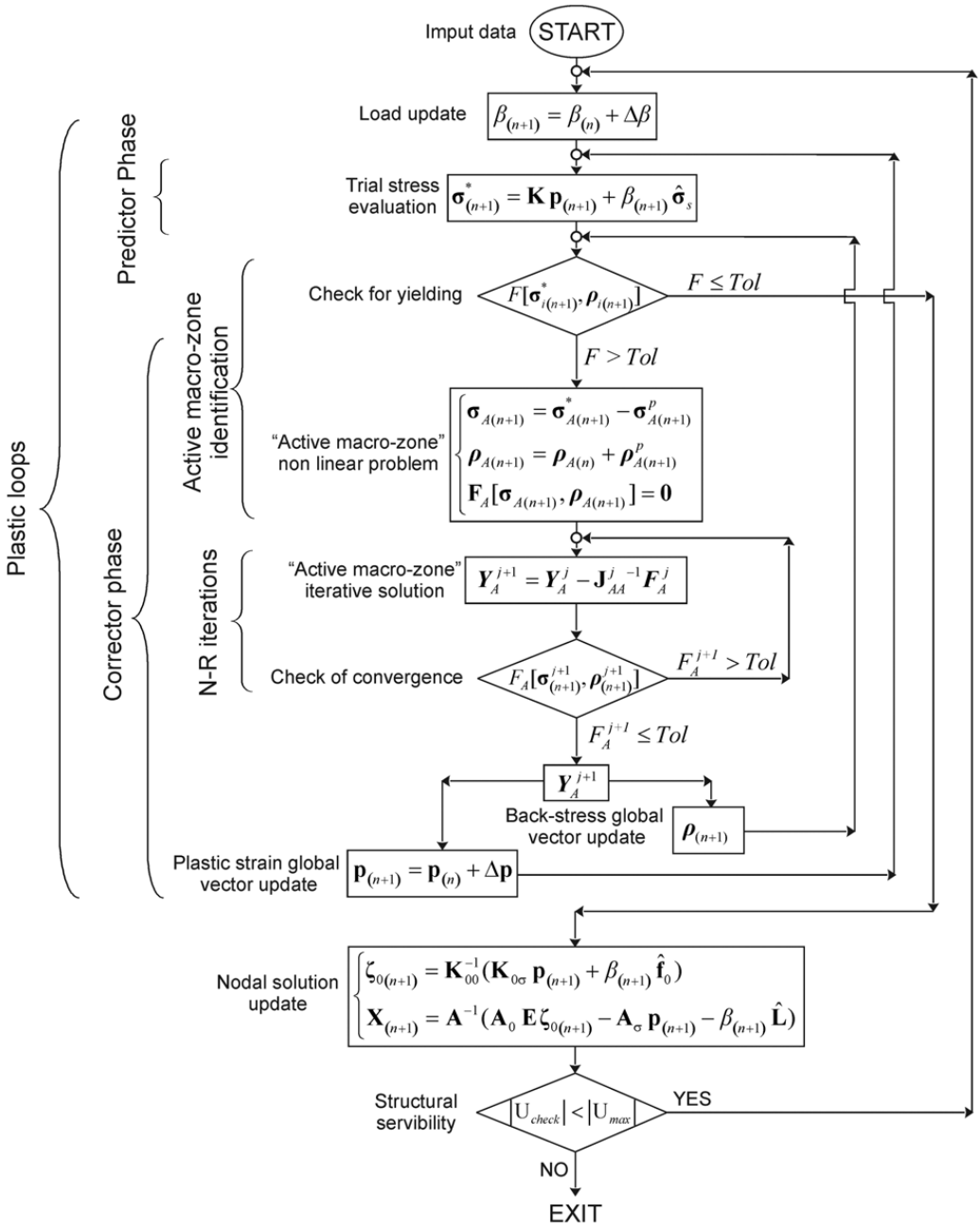

Fig. 1. Flow chart of the elastoplastic procedure.

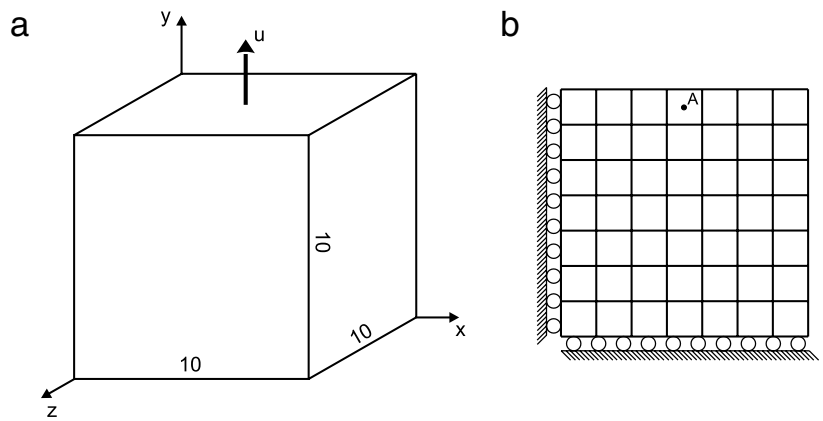

Fig. 2. Cube under imposed displacement: (a) geometric descriptions; (b) mesh adopted.

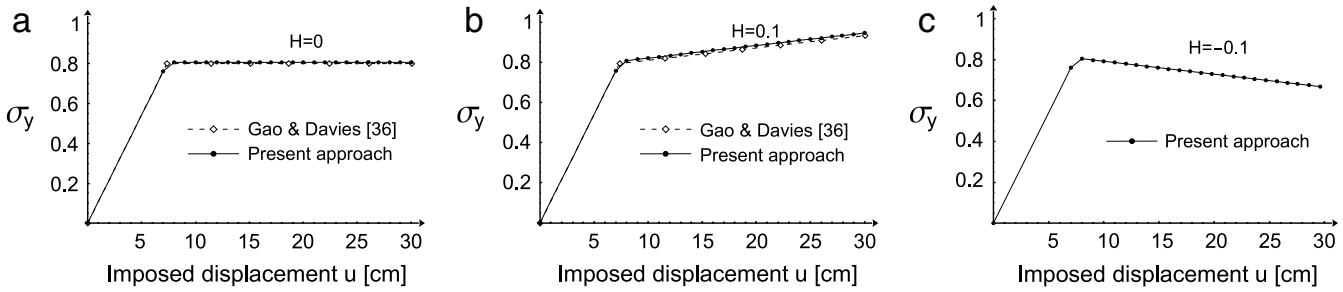

Fig. 3. Vertical stress-imposed displacement curves: (a) perfect plasticity; (b) hardening; (c) softening.

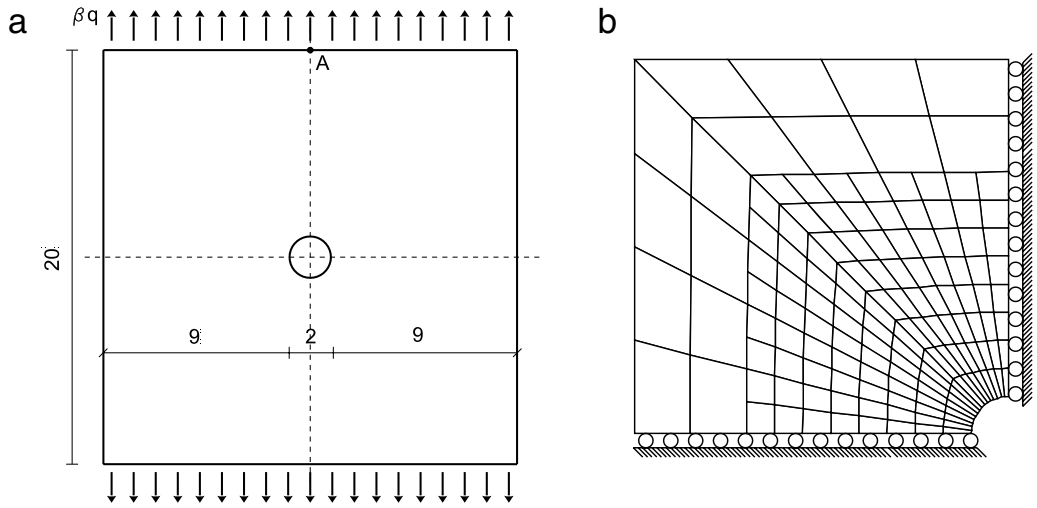

Fig. 4. Thin square plates with circular holes: (a) geometric descriptions; (b) mesh adopted.

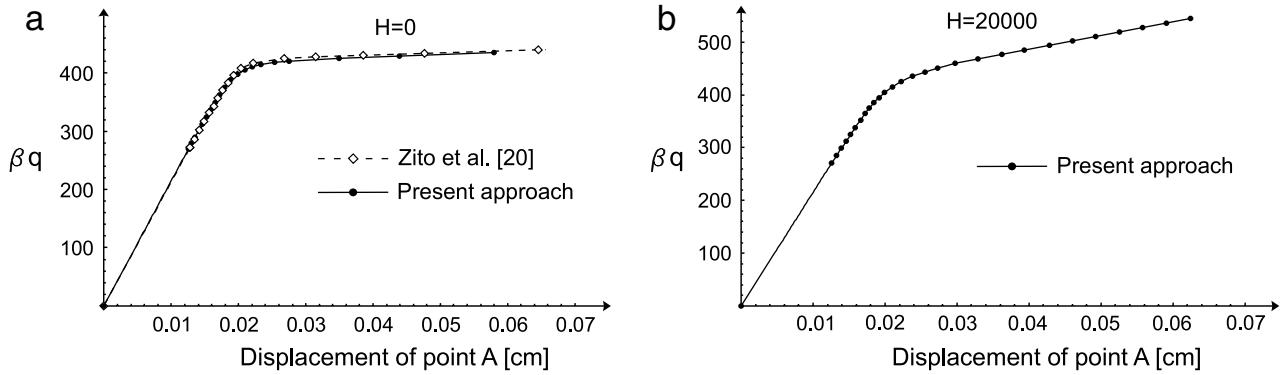

Fig. 5. Load factor-displacement curves: (a) perfect plasticity; (b) hardening.

the boundary quantities. The material characteristics are: Young's modulus $E = 206\,700$ MPa and Poisson's ratio $\nu = 0.29$, whereas the uniaxial yield value is $\sigma_y = 450$ MPa. Further in the return mapping analysis tolerance $Tol = 0.001$ was chosen.

The aim is to perform the elastoplastic analysis through two different simulations: the first in the hypothesis of perfect plasticity ($H = 0$), and the second in the hypothesis of kinematical hardening ($H = 20\,000$). In Fig. 5 the load β-displacement curves of point A, both in the perfect plasticity hypothesis and kinematical hardening one, are shown. The first was compared with the solution obtained by Zito et al. [20] inside the SGBEM for a strongly iterative approach. In treating this example the computational gain using the macro-zone strategy was 63%, but we believe that this gain is due to the example dealt with.

In Fig. 6 the N–R solution convergence in terms of vertical stress σ_y and plastic multiplier increment $\Delta\Lambda$ evaluated at the Gauss point of the bem-e near to the hole, both in the perfect plasticity hypothesis (Fig. 6a, b) and kinematical hardening one (Fig. 6c,d), are shown for load factor $\beta = 4$. In all the bem-elements the solution is obtained by few N–R iterations, generically three for each load step.

In the perfect plasticity hypothesis the load multiplier attains the value $\beta = 4.235$.

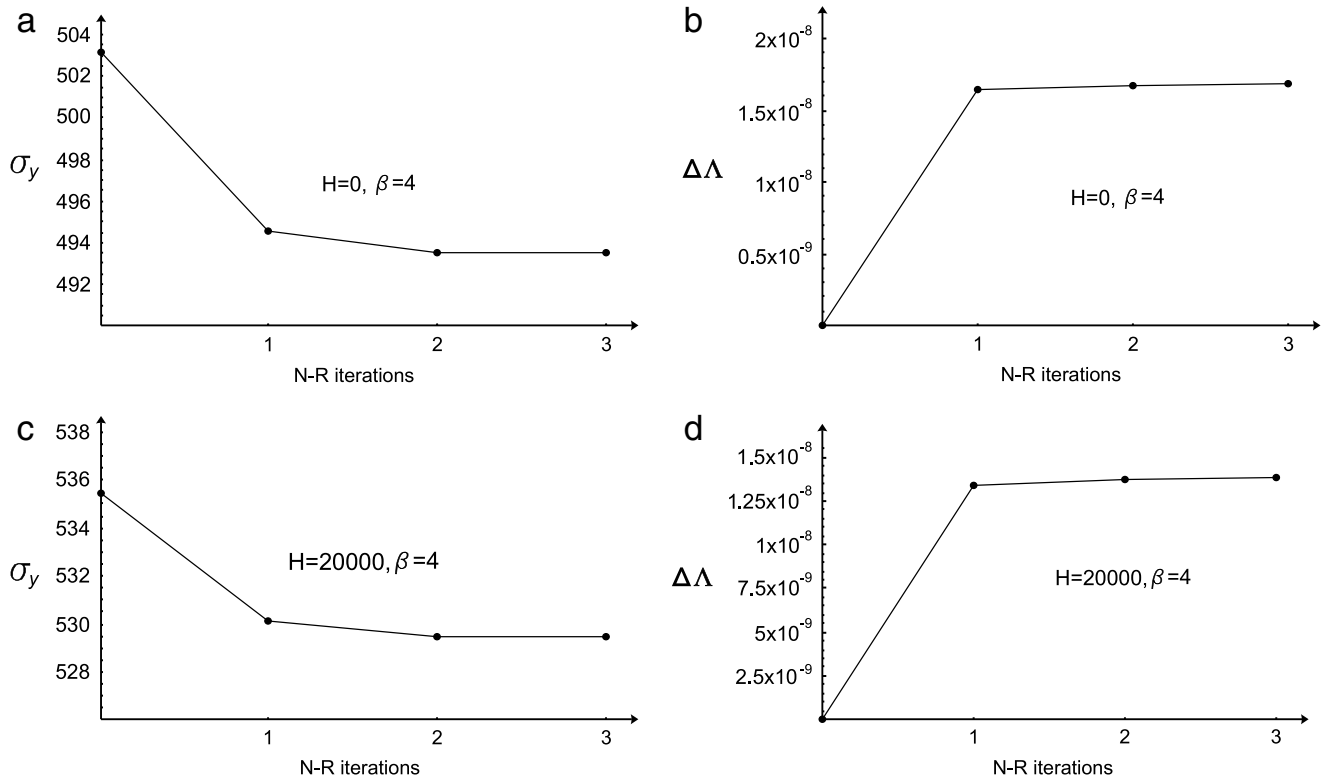

Fig. 6. N–R solutions: (a, c) vertical stress; (b, d) plastic multiplier increment.

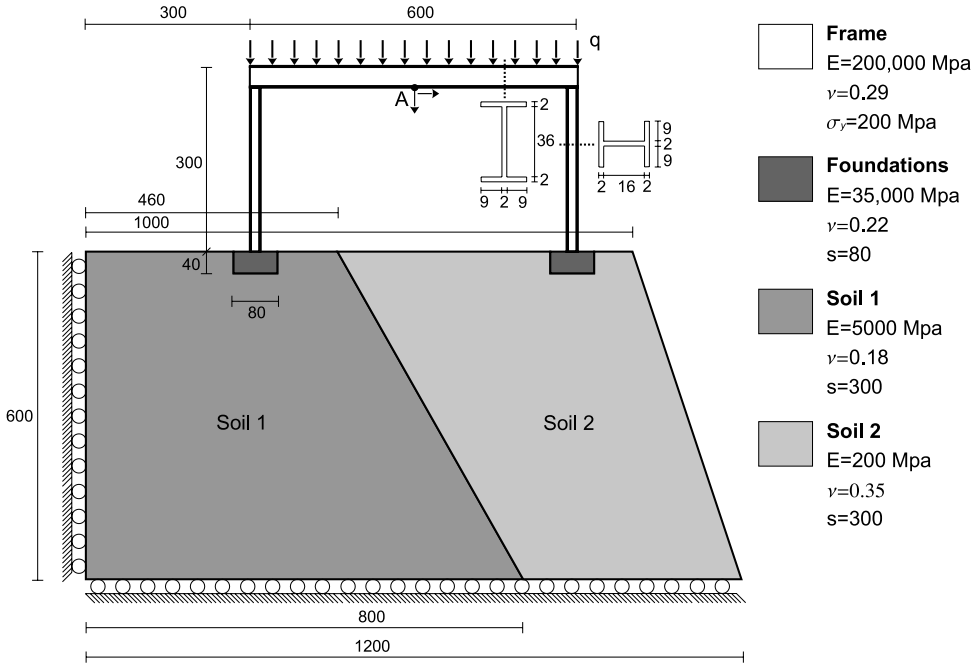

Fig. 7. Frame supported by non-homogeneous soils: geometric description.

6.3. Frame supported by non-homogeneous soil

In this example an elastoplastic plane frame, characterized by a double T-section, is located on non-homogeneous soil. The material characteristics and the geometric are shown in Fig. 7, where the dimensions are expressed in cm and "s" is the thickness of the substructures. The external action is a load uniformly distributed along all the beam with $q = 200$ kN/m as the initial value. Further, the same tolerance $Tol = 0.001$ was also chosen in this application. This system consists of a steel perfectly plastic frame, two concrete plinths and two different kinds of soil with an elastic ratio between moduli of 25. The constitutive behaviour of the concrete blocks and of the soil regions are linear elastic.

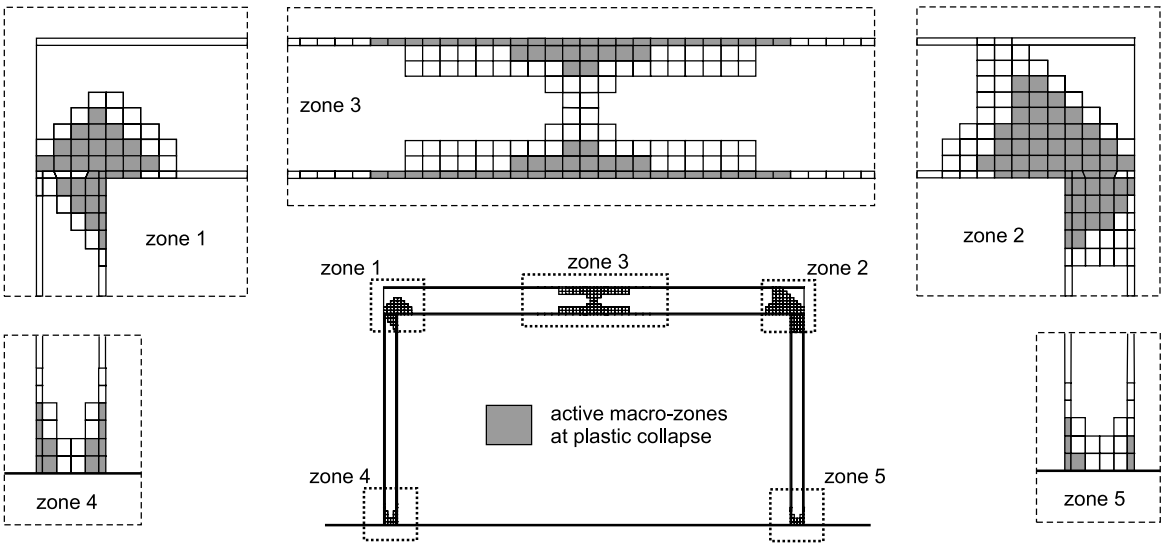

Fig. 8. Adopted mesh of the frame.

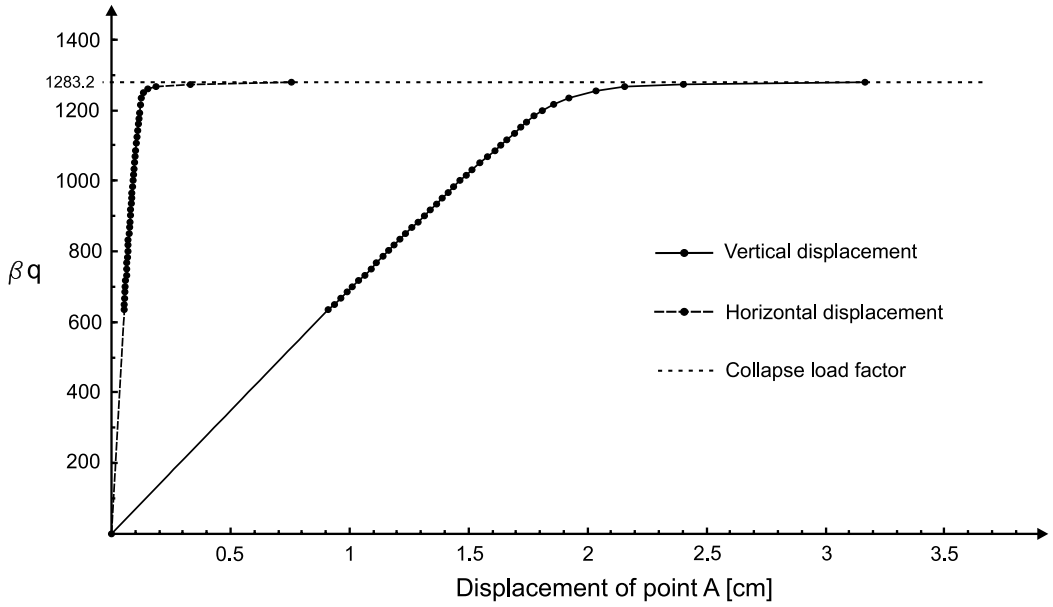

Fig. 9. Load-vertical and horizontal displacement curves of point A.

In this test first a previous purely elastic analysis of all the system, using the procedure developed by Panzeca et al. [14,15], is performed. It permits one to evaluate the stress state related to the initial load value and, as a consequence, to locate the macro-zones potentially involved by plastic strains where it is appropriate to intervene through the mesh formed by bem-elements, as reported in Fig. 8. It is important to emphasize that in order to define the optimal mesh it is sufficient to use one or leastwise two trial meshes. Indeed, this strategy locates the potentially active macro-zones, which cause the collapse of the structure, by an elastic analysis to define the zone that has to be discretized. Then the chosen mesh has to be verified by an elastoplastic analysis amplifying the range where plastic activation is possible. In Fig. 8 the active macro-zones at plastic collapse emphasized in grey. The strategy offers the great advantage of studying the remaining zone of the structure, i.e. that having elastic behaviour, as unique macroelements without domain discretization.

In Fig. 9 the load–displacement curves related to the middle point A of the frame in Fig. 7 are shown. In detail the curves regard both vertical and horizontal displacement during the loading process. Further, the plastic collapse load value $\beta q = 6.41 \cdot 200 = 1283.2$ kN/m is shown. It is to be noted that for this limit load value point A is subjected to displacement whose components increase without any limit.

In the presence of the collapse load in Fig. 10a the strained shape, obtained by enlarging the values of all the node displacements deduced from the analysis problem, and in Fig. 10b the normal stress distributions in the soil, for different depths, are shown.

In Fig. 10c, d the principal compression stress maps of the soil related to two different load instants are drawn. The first (Fig. 10c) regards the stress state for initial load $\beta q = 200$, and the second one (Fig. 10d) the stress state for the collapse

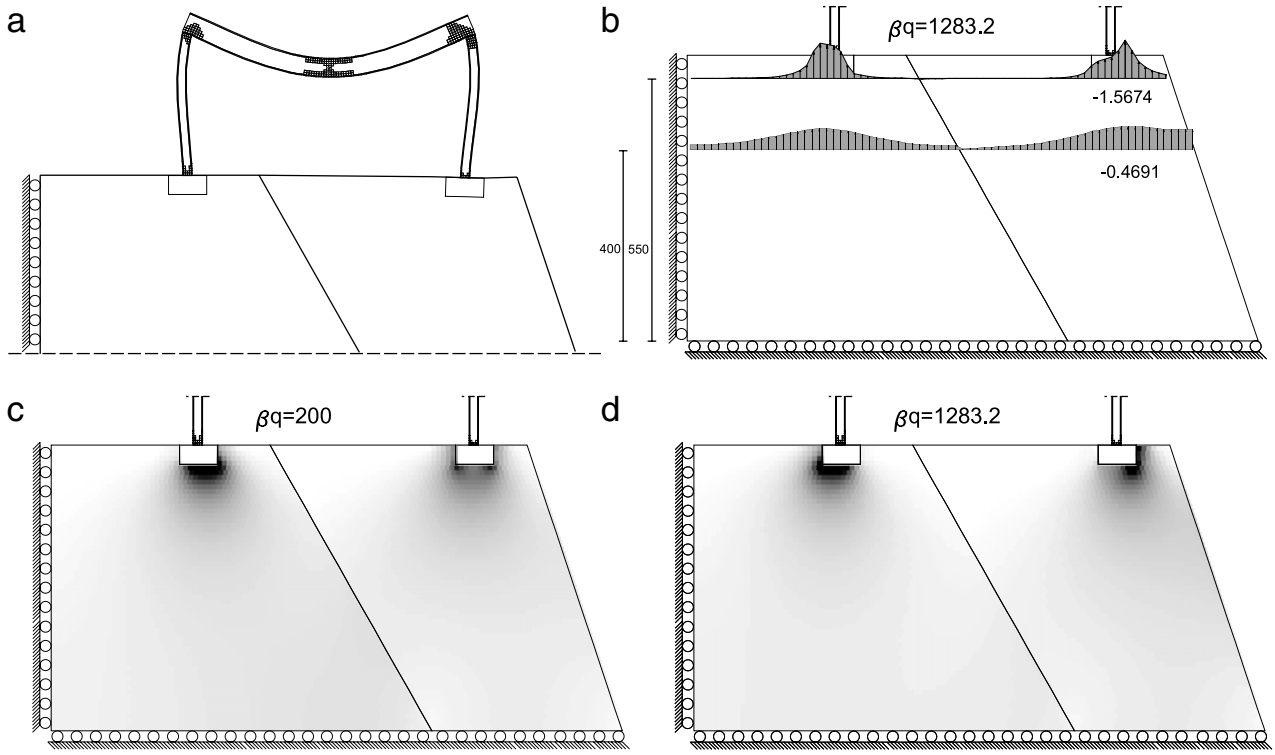

Fig. 10. (a) Deformed shape at plastic collapse; (b) stress distributions of the soils at plastic collapse; (c, d) mapping of principal compression stresses for the initial and final load factors.

load $\beta q = 1283.2$. From comparison between the two pictures it can be deduced that the plastic phenomenon in the frame changes the stress state of the soil.

This application also shows a very important advantage of this strategy, which allows one to introduce in the frame a domain discretization exclusively in the zones of potential storage of the plastic strains, leaving the rest of the structure having elastic behaviour governed by macroelements with few boundary variables.

7. Conclusions

A new strategy which couples the SGBEM with a return mapping scheme in elastoplasticity is shown in this paper. Attention has mainly been addressed to the case of homogeneous and non-homogeneous bi-dimensional solids in the hypothesis of utilizing von Mises law linear kinematic hardening and plane strain state, but the generality of this methodology makes it possible to apply it to more complex plastic models.

The elastic analysis was performed using the SGBEM for multidomain type problems, in detail called "mixed interface variable method" [13,15], which ensures the compatibility and equilibrium at all the points of the domain and in discrete form (nodal and generalized regularity conditions) on the interface boundaries. This method makes it possible to obtain a self-equilibrium stress equation to solve the elastoplastic problem regarding all the plastically active bem-elements, the latter consisting in the active macro-zones. The use of active macro-zones gives rise to a nonlocal approach which is characterized by a decrease in the plastic loops. The presence of a Jacobian operator of large dimensions involves an inversion whose computational burden is reduced through an appropriate strategy.

Moreover, the use of the SGBEM dealt with through a multidomain strategy allows one to introduce domain discretization exclusively in the zones of potential storage of plastic strains, leaving the rest of the structure as elastic macroelements, which are therefore governed by few boundary variables. This aspect makes the strategy proposed extremely advantageous.

In order to prove the efficiency of the proposed strategy, some numerical tests, performed using the Karnak.sGbem code [30], are shown.

References

[1] J.J. Perez-Gavilan, M.H. Aliabadi, A symmetric Galerkin BEM for multi-connected bodies: a new apprach, Eng. Anal. Bound. Elem. 25 (2001) 633–638.
[2] M.H. Aliabadi, D. Martin, Boundary element hyper-singular formulation for elastoplastic contact problem, Int. J. Numer. Methods Eng. 48 (2000) 995–1014.
[3] G.D. Hatzigeorgeou, D.E. Beskos, Dynamic elastoplastic analysis for 3-D structures by domain/boundary element method, Comput. Struct. 80 (2002) 339–347.
[4] T.S.A. Ribeiro, G. Beer, C. Duenser, Efficient elastoplastic analysis with boundary element method, Comput. Mech. 41 (2008) 715–732.
[5] C.A. Brebbia, J.C.F. Telles, L.C. Wrobel, Boundary Eelement Techniques, Springer-Verlag, Berlin, 1984.

[6] G. Maier, M. Diligenti, A. Carini, A variational approach to boundary element elastodynamic analysis and extension to multidomain problems, Comput. Methods Appl. Mech. Engrg. 92 (1991) 192–213.
[7] L.J. Gray, G.H. Paulino, Symmetric Galerkin boundary integral formulation for interface and multi-zone problems, Int. J. Numer. Methods Eng. 40 (1997) 3085–3101.
[8] J.B. Layton, S. Ganguly, C. Balakrishna, J.H. Kane, A symmetric Galerkin multi-zone boundary element formulation, Int. J. Numer. Methods Eng. 40 (1997) 2913–2931.
[9] S. Ganguly, J.B. Layton, C. Balakrishna, J.H. Kane, A fully symmetric multi-zone Galerkin boundary element method, Int. J. Numer. Methods Eng. 44 (1999) 991–1009.
[10] G. Maier, C. Polizzotto, A Galerkin approach to boundary element elastoplastic analysis, Comput. Methods Appl. Mech. Engrg. 60 (1987) 175–194.
[11] C. Polizzotto, An energy approach to the boundary element method, part I: elastic solids, Comput. Methods Appl. Mech. Engrg. 69 (1988) 167–184.
[12] C. Polizzotto, An energy approach to the boundary element method, part II: elastic–plastic solids, Comput. Methods Appl. Mech. Engrg. 69 (1988) 263–276.
[13] T. Panzeca, M. Salerno, Macro-elements in the mixed boundary value problems, Comput. Mech. 26 (2000) 437–446.
[14] T. Panzeca, F. Cucco, S. Terravecchia, Symmetric boundary element method versus finite element method, Comput. Methods Appl. Mech. Engrg. 191 (2002) 3347–3367.
[15] T. Panzeca, M. Salerno, S. Terravecchia, Domain decomposition in the symmetric boundary element method analysis, Comput. Mech. 28 (2002) 191–201.
[16] S. Terravecchia, Revisited mixed-value method via symmetric BEM in the substructuring approach, Eng. Anal. Bound. Elem. 36 (2012) 1865–1882.
[17] T. Panzeca, S. Terravecchia, L. Zito, Computational aspects in 2D SBEM analysis with domain inelastic actions, Int. J. Numer. Methods Eng. 82 (2010) 184–204.
[18] T. Panzeca, M. Salerno, S. Terravecchia, L. Zito, The symmetric boundary element method for unilateral contact problems, Comput. Methods Appl. Mech. Engrg. 197 (2008) 2667–2679.
[19] T. Panzeca, L. Zito, S. Terravecchia, Internal spring distribution for quasi brittle fracture via symmetric boundary element method, Eur. J. Mech. A 28 (2009) 354–367.
[20] L. Zito, E. Parlavecchio, T. Panzeca, On the computational aspects of a symmetric multidomain BEM approach for elastoplastic analysis, J. Strain Anal. 46 (2011) 103–120.
[21] T. Panzeca, Shakedown and limit analysis by the boundary integral equation method, Eur. J. Mech. A 11 (1992) 685–699.
[22] X. Zhang, Y. Liu, Y. Zhao, Z. Cen, Lower bound limit analysis by the symmetric Galerkin boundary element method and complex method, Comput. Methods Appl. Mech. Engrg. 191 (2002) 1967–1982.
[23] P.K. Banerjee, The Boundary Element Method in Engineering, McGraw Hill, London, 1994.
[24] M. Bonnet, S. Mukherjee, Implicit BEM formulations for usual and sensitivity problems in elastoplasticity using the consistent tangent operator concept, Int. J. Solids Struct. 33 (1996) 4461–4480.
[25] X.W. Gao, T.G. Davies, An effective boundary element algorithm for 2D and 3D elastoplastic problem, Int. J. Solids Struct. 37 (2000) 4987–5008.
[26] V. Mallardo, C. Alessandri, Arc-length procedures with BEM in physically nonlinear problems, Eng. Anal. Bound. Elem. 28 (2004) 547–559.
[27] C.B. Wang, J. Chatterjee, P.K. Banerjee, An efficient implementation of BEM for two- and three-dimensional multi-region elastoplastic analyses, Comput. Methods Appl. Mech. Engrg. 196 (2007) 829–842.
[28] L. Zito, F. Cucco, E. Parlavecchio, T. Panzeca, Incremental elastoplastic analysis for active macro-zones, Int. J. Numer. Methods Eng. 91 (2012) 1365–1385.
[29] T. Panzeca, E. Parlavecchio, L. Zito, X.W. Gao, X. Guo, Lower bound limit analysis by BEM: convex optimization problem and incremental approach, Eng. Anal. Bound. Elem. 37 (2013) 558–568.
[30] F. Cucco, T. Panzeca, S. Terravecchia, The program Karnak.sBem, Release 2.1, 2002.
[31] M. Bonnet, Regularized direct and indirect symmetric varational BIE formulation for three-dimensional elasticity, Eng. Anal. Bound. Elem. 15 (2005) 93–102.
[32] A. Frangi, G. Novati, Symmetric BE method in two-dimensional elasticity: evaluation of double integrals for curved elements, Comp. Mech. 19 (1996) 58–68.
[33] S. Holzer, How to deal with hypersingular integrals in the symmetric BEM, Commun. Numer. Methods Eng. 9 (1993) 219–232.
[34] S. Terravecchia, Closed form coefficients in the symmetric boundary element approach, Eng. Anal. Bound. Elem. 30 (2006) 479–488.
[35] H.D. Bui, Some remarks about the formulation of three-dimensional thermoelastoplastic problems by integral equation, Int. J. Solids Struct. 14 (1978) 935–939.
[36] X.W. Gao, T.G. Davies, Boundary Element Programming in Mechanics, Cambridge University Press, Cambridge, UK, 2002.
[37] T. Panzeca, S. Terravecchia, L. Zito, Computational aspects in thermoelasticity by the symmetric boundary element method, in: IX International Conference on Boundary Element Techniques, Seville, Spain, 2008, pp. 355–362.
[38] J. Simo, T.J.R. Hughes, Computational Inelasticity, Springer-Verlag, New York, US, 1998.
[39] M. Ortiz, J.B. Martin, Symmetry-preserving return mapping algorthms and incrementally extremal paths: a unification of concepts, Int. J. Numer. Methods Eng. 28 (1989) 1839–1853.
[40] A. Bilotta, R. Casciaro, A high-performance element for the analysis of 2D elastoplastic continua, Comput. Methods Appl. Mech. Engrg. 196 (2007) 818–828.